PSFC/JA-07-14

A Family of Analytic Equilibrium Solutions for the Grad-Shafranov Equation

Luca Guazzotto and Jeffrey P. Freidberg

MIT Plasma Science and Fusion Center,
167 Albany Street, Cambridge, MA 02139, U.S.A.

This work was supported by the U.S. Department of Energy, Grant No. DE-FG02-91ER-54109.

Accepted for publication in the Physics of Plasma (November 2007)

A family of analytic equilibrium solutions for the Grad-Shafranov equation

L. Guazzotto J. P. Freidberg

Plasma Science and Fusion Center,
Massachusetts Institute of Technology
Cambridge, Massachusetts 02139

Abstract

A family of exact solutions to the Grad-Shafranov equation, similar to those described by Atanasiu *et al.* [C. V. Atanasiu, S. Günter, K. Lackner, I. G. Miron, Phys. Plasmas **11** 3510 (2004)], is presented. The solution allows for finite plasma aspect ratio, elongation and triangularity, while only requiring the evaluation of a small number of well-known hypergeometric functions. Plasma current, pressure and pressure gradients are set to zero at the plasma edge. Realistic equilibria for standard and spherical tokamaks are presented.

I Introduction

In this work we derive a set of analytic equilibria satisfying the Grad-Shafranov (GS) equation [1]-[3] which are applicable to the tokamak configuration. The equilibria include the effects of finite aspect ratio, finite beta, and a noncircular cross section. They are also characterized by zero current and zero pressure gradient at the plasma surface, thereby making them more experimentally relevant than the well known Solovev equilibrium [4]. Recall that Solovev's equilibrium is characterized by finite jumps of pressure gradient and plasma current at the plasma surface.

The solutions are mathematically similar to those presented by Atanasiu *et al.* [5]. However, the philosophy is quite different. Atanasiu *et al.* construct equilibria by summing over an infinite set of separable solutions in the cylindrical variables (R, Z). The expansion coefficients in their sum are determined by requiring that the boundary condition $\Psi = const.$ be satisfied on a pre-specified plasma shape. This is a useful approach when trying to compare with experimental data.

In our approach we use just three terms in the infinite set of separable solutions. Thus, while we cannot specify a precise plasma shape, we do have the freedom to specify certain macroscopic properties related to the cross section, in particular the major and minor radii, the elongation, and the triangularity. The solutions therefore are mathematically simple and because they are analytic they (1) serve as good benchmarks for testing numerical magnetohydrodynamics (MHD) equilibrium codes and (2) provide a good model to test for stability without having to worry about accuracy and resolution issues arising from numerically computed equilibria. In fact, we have benchmarked our analytic solution against the equilibrium code FLOW [6] for several cases,

including highly-shaped, tight aspect ratio equilibria, with excellent agreement between the two.

To summarize, the main contribution of the paper is the derivation of simple, analytic tokamak equilibria with realistic edge conditions that can be easily evaluated using any of the standard computational packages such as Mathematica.

The paper is organized as follows. In Section II we derive the general analytic solutions to the Grad-Shafranov equation using our specific choices for the free functions. Section III describes the strategy used to determine the finite number of unknown expansion coefficients in the three term solution. We also compare our approach with that of Atanasiu *et al.* In Section IV we apply the results to several experiments of interest, specifically the National Spherical Torus Experiment (NSTX) [7], ITER [8] and ARIES-ST (Spherical Torus) [9]. Lastly, in Section V we carry out an exploration of the equilibrium parameter space with the goal of deriving some simple empirical relations that define where in this parameter space the interesting equilibria exist.

II The general equilibrium solution

Tokamak equilibria are described by the well known Grad-Shafranov equation [1]-[3] given by

$$\Delta^* \Psi = -\mu_0 R^2 \frac{dp}{d\Psi} - \frac{1}{2}\frac{dF^2}{d\Psi}, \tag{1}$$

where $\Delta^* \Psi \equiv R^2 \nabla \cdot \left(\nabla \Psi / R^2\right)$ and the magnetic field is related to the poloidal flux Ψ by:

$$B_\varphi = \frac{F(\Psi)}{R}, \tag{2}$$

$$\boldsymbol{B}_p = \frac{\nabla \Psi \times \boldsymbol{e}_\varphi}{R}. \tag{3}$$

We choose the free functions $p(\Psi)$ and $F(\Psi)$ to be quadratic in Ψ as also suggested by Atanasiu *et al.* Specifically we set

$$\begin{aligned} p &= p_{axis}\left(\Psi^2/\Psi_{axis}^2\right) \\ F^2 &= R_0^2 B_0^2\left[1 + b_{axis}\left(\Psi^2/\Psi_{axis}^2\right)\right]. \end{aligned} \tag{4}$$

Here Ψ_{axis}, p_{axis} and b_{axis} are constants related to the values of Ψ, p and F on axis and R_0 and B_0 are the major radius and vacuum toroidal field at the geometric center of the plasma. Note that for a vacuum toroidal field $b_{axis} = 0$ and $B_\varphi = B_0(R_0/R)$. With plasma pressure the toroidal field is given by $B_\varphi = B_0(R_0/R)(1 + b_{axis}\Psi^2/\Psi_{axis}^2)^{1/2}$. On the magnetic axis $R = R_{axis}$, $\Psi = \Psi_{axis}$, giving $B_\varphi = B_{axis}(1 + b_{axis})^{1/2}$. Here $B_{axis} = B_0(R_0/R_{axis})$ is the vacuum field at $R = R_{axis}$. We see that b_{axis} is a measure of the plasma diamagnetism (if $b_{axis} < 0$) or paramagnetism (if $b_{axis} > 0$).

The Grad-Shafranov equation reduces to

$$\Delta^*\Psi = -\frac{R_0^2 B_0^2}{\Psi_{axis}^2}\left(b_{axis} + \beta_{axis}\frac{R^2}{R_0^2}\right)\Psi, \tag{5}$$

where $\beta_{axis} = 2\mu_0 p_{axis}/B_0^2$. The choice of free functions given above has the advantage of making the Grad-Shafranov equation a *linear* partial differential equation.

The next step is to introduce normalized variables: $\Psi = \Psi_{axis}\psi$, $R^2 = R_0^2 x$, and $Z = ay$, with a being the minor radius of the plasma. Equation (5) can then be rewritten as

$$4\epsilon^2 x\frac{\partial^2\Psi}{\partial x^2} + \frac{\partial^2\Psi}{\partial y^2} + (\alpha x + \gamma)\Psi = 0, \tag{6}$$

where $\epsilon = a/R_0$ and

$$\begin{aligned} \gamma &= \left(\frac{aR_0B_0}{\Psi_{axis}}\right)^2 b_{axis} \\ \alpha &= \left(\frac{aR_0B_0}{\Psi_{axis}}\right)^2 \beta_{axis}. \end{aligned} \tag{7}$$

The solution to Eq. (6) is found by separation of variables:

$$\psi = \sum_m X_m(\rho) Y_m(y), \tag{8}$$

where $x = -i(\epsilon/\sqrt{\alpha})\rho$. The Y_m equation and its solution for an up-down symmetric configuration is given by:

$$\begin{aligned} \frac{d^2 Y_m}{dy^2} + k_m^2 Y_m &= 0 \\ Y_m(y) &= \cos(k_m y). \end{aligned} \tag{9}$$

Here, k_m is the m^{th} separation constant, which can be real or imaginary and is as yet undetermined. In the non-symmetric case, $Y_m(y) = c_m \cos(k_m y) + d_m \sin(k_m y)$. Some more details on the non-symmetric case are given later.

The $X_m(\rho)$ equation reduces to:

$$\frac{d^2 X_m}{d\rho^2} + \left[-\frac{1}{4} + \frac{\lambda_m}{\rho} \right] X_m = 0, \tag{10}$$

with

$$\lambda_m = -i \frac{\gamma - k_m^2}{4\epsilon\sqrt{\alpha}}. \tag{11}$$

The solutions for $X_m(\rho)$ of Eq. (10) are Whittaker functions [10], whose mathematical properties are well known and which can be easily evaluated numerically using, for instance, Mathematica:

$$X_m(\rho) = a_m W_{\lambda_m,\mu}(\rho) + b_m M_{\lambda_m,\mu}(\rho). \tag{12}$$

The a_m and b_m are unknown expansion coefficients and for our model the Whittaker parameter $\mu = 1/2$.

The mathematical properties of the solution are slightly subtle, since both ρ and λ_m are purely imaginary quantities, while X_m must be purely real. The subtleties can be resolved by setting $\rho = iz$, $\lambda_m =$

$i\Lambda_m$ and noting the following properties of the Whittaker functions for $\mu = 1/2$:

$$M_{\lambda_m,1/2}(\rho) = \rho M(\lambda_m\rho, \lambda_m^2) = izM(-\Lambda z, -\Lambda_m^2) \tag{13a}$$

$$\begin{aligned} W_{\lambda_m,1/2}(\rho) &= \rho ln(\rho) M(\lambda_m\rho, \lambda_m^2) + \lambda_m W(\lambda_m\rho, \lambda_m^2) \\ &= iz(lnz + i\frac{\pi}{2})M(-\Lambda_m z, -\Lambda_m^2) + i\Lambda_m W(-\Lambda_m z, -\Lambda_m^2), \end{aligned} \tag{13b}$$

where M and W are real functions for real arguments. The appearance of the $i\pi/2$ term in $W_{\lambda_m,1/2}(\rho)$ implies that the expansion coefficients must in general be complex if X_m is to be real. This difficulty can be avoided by observing that $i\pi/2$ multiplies $M_{\lambda_m,1/2}(\rho)$ and can therefore be incorporated in the a_m coefficient. The end result is that the solution for X_m can be rewritten as:

$$X_m(\rho) = Im\left[a_m W_{\lambda_m,1/2}(\rho) + b_m M_{\lambda_m,1/2}(\rho)\right], \tag{14}$$

with a_m, b_m and X_m being purely real. Hereafter, the "Im" notation is suppressed for convenience, but we must keep in mind that we only require the imaginary parts of the Whittaker functions when evaluating them numerically.

Equation (8) represents the general mathematical solution to the Grad-Shafranov equation in R, Z coordinates. For a boundary condition we require that $\psi = 0$ on the plasma surface. Note that the boundary condition implies that p, ∇p and J_φ vanish on the plasma surface.

Atanasiu *et al.* arrive at a similar solution, but slightly more general, since they allow for linear terms in the definitions in Eq. (4), which produce jumps in J_φ and ∇p on the surface. Their approach to determine equilibria is to specify a desired shape for the plasma

surface and to then choose the infinite set of a_m, b_m, and k_m to match the boundary condition. Note that there is no guarantee that such an expansion will *always* converge since the coordinates (R, Z) used in the separation of variable solutions are in general not natural to the shape of the surface. An analogy is to try and solve $\nabla^2\psi = 0$ on a 2-D circular cylinder, not by using the natural polar coordinates (r, θ), but instead using the sinusoidal and exponential solutions associated with the rectangular coordinates (x, y). Sometimes this works, most other times it doesn't.

The convergence difficulty appears mathematically in the Atanasiu *et al.* solution as follows. For a general plasma shape there is no natural or obvious way to choose the separation constants k_m. Some cleverness and intuition are required to select appropriate values. In spite of this potential difficulty Atanasiu *et al.* do find interesting regimes of parameter space describing realistic plasma equilibria by using a large number of values for k_m ($m_{MAX} \sim 30$).

Our approach is different. We attempt to find interesting solutions by keeping only a small, finite number of terms in the infinite series. The minimum number is found empirically to be three terms. The free constants (of which there are now a finite number) are chosen to satisfy certain macroscopic constraints, such as aspect ratio, elongation, triangularity, etc. The actual shape of the plasma is found by simply plotting the resulting curve $\psi(R, Z) = 0$. This approach also faces the convergence difficulty described above. Over certain ranges of parameters the plasma shape satisfies the specified geometric constraints at the corresponding finite number of locations but its overall shape is quite distorted from what one would like. An example of this problem is given shortly. In any event we have been able to identify regions of

parameter space that are of experimental interest including the effects of both high β and tight aspect ratio.

We now describe in more detail how to calculate the coefficients in the three term solution.

III Solution strategy

The solution given by Eq. (8) is a correct mathematical solution of the GS equation for any value of the separation constant, and of the parameters α and γ. However, in order to obtain a solution with magnetic geometry appropriate to a specific problem, a special choice is required for the parameters and separation constant(s). The focus of the remainder of this work is on tokamak-relevant solutions. Even though the exact plasma shape cannot be assigned in our solution, we show in the following that good approximations to realistic tokamak shapes can be obtained. In general, we will define to be "good" equilibria where the difference between the input shape and the boundary shape is small enough. More precisely, in a "good" equilibrium the error defined later in Eq. (24) will be $\lesssim 1\%$; moreover, we also require the equilibrium to have only one maximum of ψ inside the boundary. Clearly, the "goodness" of an equilibrium depends on the input plasma shape: equilibria which are good for some applications may be bad for others, and vice versa.

The first step in the solution procedure is to specify the inputs to the problem. The primary inputs are the inverse aspect ratio ϵ, the elongation κ, the triangularity δ, and the parameters α and γ. The first three are geometric parameters with their usual meaning as illustrated in Fig. 1. The parameters α and γ also have physical meanings, with

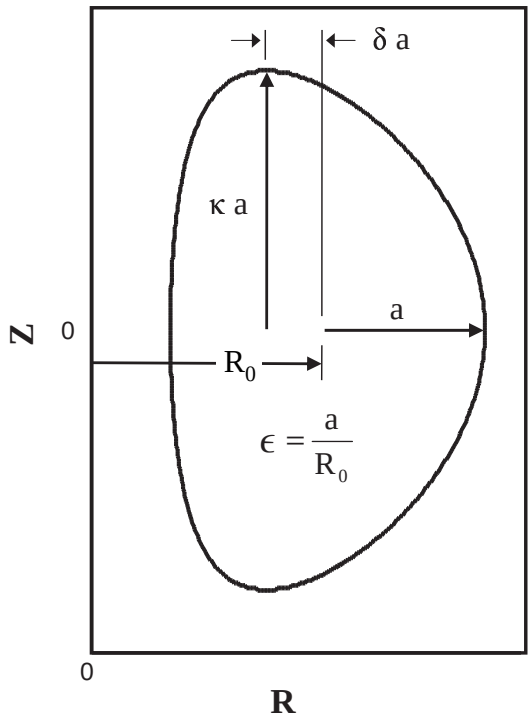

Figure 1: Definition of the dimensionless geometric parameters.

$\alpha \sim \beta_p$, where β_p is the poloidal beta, and $\gamma \sim 2(q/\epsilon)^2 (\delta B_\varphi / B_\varphi)$ is the normalized diamagnetism. These connections to the physical quantities of interest make it possible to choose reasonable values for α and γ.

The secondary input parameters of interest are the major radius R_0, the vacuum toroidal field B_0, and the toroidal current I. The quantities B_0 and R_0 are scaling parameters and thus can be chosen freely. The current I can also be chosen freely by adjusting the value of Ψ_{axis}, which is a free parameter. Alternatively, rather than specifying

I one can give a single value of the safety factor, for instance q_{axis}, q_{edge}, or $q_* = 2\pi a^2 \kappa B_0/(\mu_0 R_0 I)$. This can again be accomplished by adjusting the value of Ψ_{axis}, since in general the safety factor scales as $q \sim (B_0 R_0^2/\Psi_{axis}) g(\alpha, \gamma, \epsilon, \kappa, \delta)$. In the present work we assume that R_0, B_0 and either I or q_{axis} are specified when needed.

Next, we write down ψ maintaining three terms in the summation:

$$\psi(\rho, y) = \sum_1^3 \left[a_m W_{\lambda_m,1/2}(\rho) + b_m M_{\lambda_m,1/2}(\rho) \right] \cos(k_m y). \tag{15}$$

Observe that there are six unknown expansion coefficients (i.e. the a_m, b_m) and three unknown separation constants (i.e. the k_m). The coefficients are determined as follows.

Two conditions follow from fixing the inner and outer midplane surface points at the desired locations:

$$\Psi(R_0 + a, 0) = 0 \tag{16a}$$

$$\Psi(R_0 - a, 0) = 0. \tag{16b}$$

Two conditions are needed to define the point of maximum surface elongation:

$$\Psi(R_0 - \delta a, \kappa a) = 0 \tag{17a}$$

$$\Psi_R(R_0 - \delta a, \kappa a) = 0. \tag{17b}$$

Our empirical experience shows that it helps substantially to make sure that the surface has the right convexity on the inboard midplane. A simple way to do this is to consider a traditional analytical representation of the plasma surface:

$$\begin{aligned} R &= R_0 + a \cos\left[\theta + \hat{\delta} \sin(\theta)\right] \\ Z &= \kappa a \sin(\theta), \end{aligned} \tag{18}$$

where

$$\hat{\delta} = \sin^{-1}(\delta). \tag{19}$$

Evaluating and equating the inboard midplane curvature vector $\boldsymbol{e}_R/R_c$ for our solution to the traditional analytic solution leads to the following condition:

$$\frac{1}{R_c} \equiv \frac{\Psi_{ZZ}(R_0 - a, 0)}{\Psi_R(R_0 - a, 0)} = -\frac{(1 - \hat{\delta})^2}{\kappa^2 a}. \tag{20}$$

The last condition corresponds to the normalization requirement that $\psi = \Psi/\Psi_{axis} = 1$ on the magnetic axis. This actually translates into two coupled conditions, one defining the location of the magnetic axis (i.e. R_{axis}) and the other the normalization:

$$\Psi_R(R_{axis}, 0) = 0, \tag{21a}$$

$$\Psi(R_{axis}, 0) = \Psi_{axis}. \tag{21b}$$

Equations (16), (17), (20) and (21) represent seven equations for seven unknowns (i.e. the six unknown expansion coefficients plus R_{axis}).

Consider next the separation constants. These are chosen by a combination of empirical experience and general considerations. First, we observe that the simplest possible solution for Eq. (1) does not depend on Z. By setting $k_1 = 0$ we obtain $\lambda_1 = -i\gamma/(4\epsilon\sqrt{\alpha})$. No universal "good" choices for the other two constant have been identified. Several different strategies have been considered and tested over a large number of equilibria. Our empirical experience has lead us to the following approach for determining the remaining separation constants:

$$k_2 = i\hat{k}_2 \tag{22a}$$

$$k_3 = \frac{\pi}{\kappa}\hat{k}_3, \tag{22b}$$

with $\hat{k}_2$, $\hat{k}_3$ real and of order unity. This choice corresponds to having one of the $Y_m(y)$ purely growing (for $m = 2$) and one oscillating (for $m = 3$). The approach has proved to be satisfactory over a large number of equilibria, as long as appropriate values for $\hat{k}_2$, $\hat{k}_3$ are used. It turns out that the optimal (in the sense of producing the resulting geometry closest to the desired one) choice is problem-dependent, even though some general rules can be determined. More details on this issue are given in the next sections. For now, we will assume that appropriate values for $\hat{k}_2$, $\hat{k}_3$ are given once the plasma geometry has been chosen.

A summary of the conditions is written out explicitly in terms of the normalized variables in Appendix A. Finding the unknown coefficients then requires a trivial numerical calculation. Once the coefficients are determined, the solution for ψ can be written as:

$$\begin{aligned}\psi(\rho, y) =&(a_1 W_1 + b_1 M_1) + (a_2 W_2 + b_2 M_2)\cos(k_2 y) \\ &+ (a_3 W_3 + b_3 M_3)\cos(k_3 y),\end{aligned} \tag{23}$$

where $W_j \equiv W_{\lambda_j,1/2}(\rho)$ and $M_j \equiv M_{\lambda_j,1/2}(\rho)$. Hereafter, we assume that once ϵ, κ, δ, α and γ are given, then the k_m and a_m, b_m are known.

If non-symmetric equilibria are considered, one should replace $\cos(k_{2,3}y)$ with $c_{2,3}\cos(k_{2,3}y) + d_{2,3}\sin(k_{2,3}y)$. With this replacement, four more unknown coefficients must be determined. In order to do that, four additional equations must be defined on the curve $\psi = 0$. Moreover, separate values for triangularity and elongation need to be assigned for the two regions ($Z > 0$ and $Z < 0$) of the plasma.

IV Applications

In this section we apply the analytic solutions to two configurations of fusion interest: the standard tokamak (such as ITER) and the spherical tokamak (such as NSTX and ARIES-ST). We also demonstrate the difficulties with convergence to a "good" i.e. tokamak-relevant equilibrium by means of a simple example.

We first investigate the issue of convergence. As an example, consider a standard aspect ratio tokamak with a circular cross section. Three cases are examined. For each the geometric parameters are held fixed: $\epsilon = 0.3125$, $\kappa = 1$, and $\delta = 0$. Also fixed is the parameter $\gamma = -0.68$. Three values of α are tested: $\alpha = 6.11$, $\alpha = 7.21$, $\alpha = 5.65$. The corresponding values of the free separation constants are given by $k_2 = 0.096i$ and $k_3 = 2.17$. For each case the expansion coefficients are determined as outlined in Appendix A.

The resulting flux surfaces $\psi = const.$ are illustrated in Fig. 2. Observe that only the first case represents a "good" equilibrium (again, in the sense of being tokamak-relevant). The other two cases both satisfy the geometric requirements but are uninteresting equilibria.

The conclusion is as follows. The equilibrium procedure always results in a mathematical function that satisfies the original GS equation and the geometric constraints. However, "good" tokamak-like solutions are only possible over interconnected ranges of values for α, γ, k_2 and k_3. A determination of these ranges is discussed in the next section. We also point out that similarly non tokamak-relevant results are obtained if any single other parameter (γ, k_2, k_3) is changed by a sufficient amount. Moreover, observe that uninteresting results are obtained if α is changed by a relatively small amount $(10 - 20\%)$ from the optimal value.

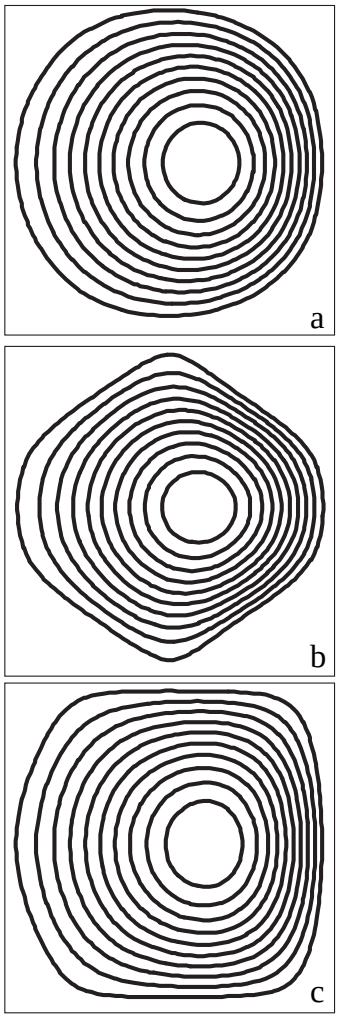

Figure 2: Magnetic surfaces for equilibria with "circular" cross section for different values of α. From top to bottom, the equilibria correspond to $\alpha = 6.11$ (a), $\alpha = 7.21$ (b) and $\alpha = 5.65$ (c). All other physical parameters are kept unchanged: $\gamma = -0.68$, $\epsilon = 0.3125$, $\delta = 0$, $\kappa = 1$, $k_2 = 0.096i$, $k_3 = 2.17$.

Table 1: Equilibrium data.

Parameter	**ITER**	**ARIES-ST**	**NSTX**	**NSTX-separatrix**
ϵ inverse aspect ratio	0.32	0.625	0.79	0.79
κ elongation	1.8	3.4	2.2	2.4
δ triangularity	0.45	0.64	0.5	0.5
α pressure parameter	4.48	3.07	3.56	3.56
γ diamagnetism parameter	-0.5	-0.05	-0.1	-0.1
k_2 second separation constant	$0.90i$	$0.012i$	$0.024i$	$0.024i$
k_3 third separation constant	1.82	1.28	1.77	1.62
B_0 toroidal field [T]	5.3	2.1	0.43	0.43
I toroidal current [MA]	10.1	11.15	0.43	0.41
R_0 major radius [m]	6.2	3.2	0.85	0.85
a minor radius [m]	2	2	0.67	0.67
β_t toroidal beta [%]	2.1	6.2	4.4	4.3
peak beta [%]	9.25	34	20.6	20.1
q_{axis} safety factor on axis	1	1	1	1
q_{95} safety factor at 95 % flux	4.8	12.3	19	18
q_* kink safety factor	3.1	4.0	5.9	6.6

Next we shall calculate equilibria describing a standard ITER-like tokamak, a spherical NSTX-like spherical tokamak and an ARIES-ST-like spherical tokamak. For the NSTX case we also show an equilibrium with a separatrix. The input parameters for these cases are listed in Table 1. As one can see from the table, reasonable plasma character-

istics are obtained with the analytic solution for all cases presented. The shapes of the resulting equilibria are shown in Fig. 3. Dotted

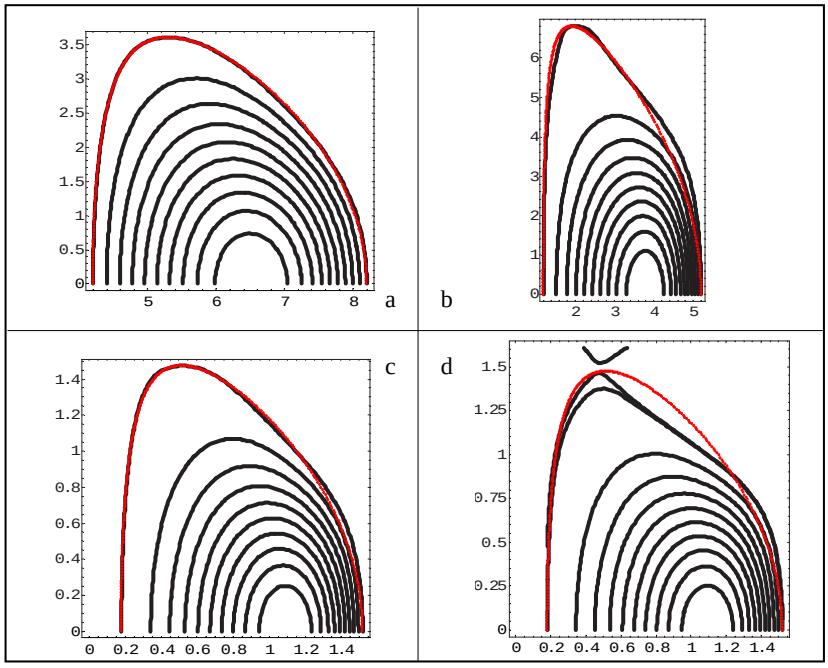

Figure 3: (Color online) Plasma shape for four analytic equilibria: ITER-like (a), ARIES-ST-like (b), NSTX-like (c) and NSTX-like with separatrix (d). The dots (in color in the online version) represent the analytic shape. The same analytic shape is shown for (c) and (d). Due to up-down symmetry, in each case only half of the plasma is shown.

lines represent the "input" shape obtained from Eq. (18). We see that all boundary shapes are reasonably close to the desired one, with the standard tokamak (ITER) shape being an almost perfect match.

We now consider in more detail the ITER equilibrium. Plots of the most important physical quantities versus the major radius along

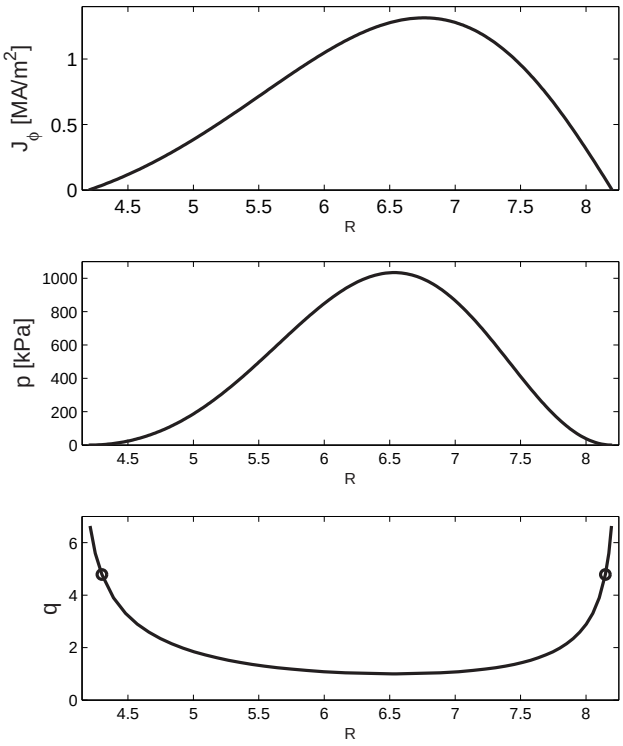

Figure 4: Physical quantities along the midplane for a "good" ITER equilibrium. From top to bottom, the following are shown: toroidal current density J_φ, pressure p and safety factor q. The circles in the q profile correspond to $q_{95} \simeq 4.8$.

the midplane are presented in Fig. 4. From top to bottom, the figure shows the toroidal current density J_φ, the plasma pressure p and the safety factor q. In the q profile, the value q_{95} has been highlighted with circles. All profiles are quite realistic. Note that the vanishing of ∇p and J_φ at the edge, combined with the linear dependence on Ψ

produces peaked pressure and currents profiles, which in turn lead to relatively low values of average β and high values of q_{edge}. However the peak values of β are quite substantial. The profiles obtained for the ARIES-ST and the NSTX equilibrium show similar behavior.

It is useful to describe in more detail the separatrix case. Although we prefer to leave the main focus of the present work on equilibria without a separatrix, it is nonetheless interesting to discuss how equilibria with an X-point can be obtained. It turns out that once an equilibrium without separatrix is given, it is a trivial task to obtain a related equilibrium with a separatrix. By keeping all input parameters constant and only increasing κ, a separatrix will appear next to the top boundary of the plasma. If κ is increased further, the separatrix will move downwards. Note that due to Eq. (22b) k_3 also changes when κ changes, since we keep $\hat{k}_3$ constant rather than k_3. The equilibrium shown in Fig. 3 (d) was obtained with the same input parameters used for the spherical torus shown in Fig. 3 (c), with the exception of the elongation, which was increased to $\kappa = 2.4$. For both equilibria, the shape obtained from Eqs. (18) for $\kappa = 2.2$ is plotted as a reference. The separatrix appearing on the top portion of the plasma is clearly visible. Also the plasma shape is still close to the analytic shape, but is not as close to it as the one in the equilibrium shown in Fig. 3 (c). In general, the farther κ is from the optimal value for matching an input shape, the farther the plasma shape moves from the input one. For that reason, one should use this approach to obtain equilibria with a separatrix only if that can be accomplished with small variations in κ. Otherwise, different values for the input parameters other than κ should also be chosen, by using the optimization approach described in the next section.

Finally, we point out that since there is no freedom in the choice of the free functions, which are given by Eq. (4), advanced tokamak features such as reversed shear cannot be reproduced with our solution. However, we have shown that realistic standard-operational parameters and profiles can be obtained.

One issue that we have not yet addressed is how to determine a good set of values for the input parameters α, γ, k_2 and k_3 for a given plasma geometry. That is discussed in the next section.

V Equilibrium parametric study

As discussed, the main limitation in the use of the analytic solution described in this work is the fact that if the input parameters α, γ, k_2 and k_3 are chosen arbitrarily, the resulting equilibrium will have a somewhat unpredictable magnetic geometry. In order to obtain an equilibrium suited for a particular application (specifically a tokamak-like equilibrium), special choices are required for the input parameters. During the course of our investigation, several different strategies have been tried.

Our experience has shown that a satisfactory procedure is to choose a value for γ (negative for a diamagnetic plasma), assume k_2 to be imaginary and k_3 real, and then determine the values of α, k_2, k_3 by minimizing an appropriate error function. A reasonable choice for the error function makes use of the traditional analytic plasma shape given by Eq. (18). Since our goal is to match the shape of our three term solution as closely as possible to the traditional shape we use the

following definition of the error function:

$$E(\alpha, k_2, k_3; \gamma) = \\ \frac{\sum_i \sqrt{[R_{3term}(\theta_i) - R_{trad}(\theta_i)]^2 + [Z_{3term}(\theta_i) - Z_{trad}(\theta_i)]^2}}{\sum_i \sqrt{R_{trad}^2(\theta_i) + Z_{trad}^2(\theta_i)}}, \tag{24}$$

where the sum typically includes 300 angles around half of the surface (due to up-down symmetry, we only need to consider $Z > 0$). Due to Eqs. (16), (17), (18) and (19) the only boundary points that are enforced in our three term solution are also points on the traditional plasma shape. For that reason it is at least in principle possible to reduce the error function to zero. That is not possible in practice; however, as shown in Section IV, the procedure does a reasonably good job reproducing the desired plasma shapes. The parameters listed in Table 1 have been determined by minimizing E using a built-in minimizing routine in Mathematica.

To avoid a time consuming and some times frustrating effort searching for appropriate input parameters we have compiled a large amount of data obtained by minimizing E over a many cases and converted the results into simple empirical fits for α, k_2, k_3 as functions of γ. We have completed this task for all geometries discussed in Section IV. Our results show that the γ dependence is not too strong and can be approximated by a quadratic polynomial. Specifically we write:

$$\begin{aligned} \alpha(\gamma) &= C_0^{(\alpha)} + C_1^{(\alpha)}\gamma + C_2^{(\alpha)}\gamma^2 \\ \hat{k}_2(\gamma) &= C_0^{(k_2)} + C_1^{(k_2)}\gamma + C_2^{(k_2)}\gamma^2 \\ \hat{k}_3(\gamma) &= C_0^{(k_3)} + C_1^{(k_3)}\gamma + C_2^{(k_3)}\gamma^2, \end{aligned} \tag{25}$$

where we have used the definitions of Eq. (22), $k_2 = i\hat{k}_2$, $k_3 = (\pi/\kappa)\hat{k}_3$. The coefficients for the approximated formulas in Eq. (25) are given in Table 2. For the NSTX case, the formula holds for $-3 \leq \gamma \leq 0$,

Table 2: Expansion coefficients in the approximated formulas for the free equilibrium parameters.

	ITER	**NSTX**	**ARIES-ST**
$C_0^{(\alpha)}$	3.99	3.49	3.03
$C_1^{(\alpha)}$	-0.985	-0.71	-0.82
$C_2^{(\alpha)}$	-8.2 10^{-3}	-0.012	-0.032
$C_0^{(k_2)}$	0.063	4.2 10^{-3}	1.6 10^{-3}
$C_1^{(k_2)}$	0.011	-0.14	-6.4 10^{-3}
$C_2^{(k_2)}$	4.4 10^{-4}	-0.042	- 1.8 10^{-3}
$C_0^{(k_3)}$	1.03	1.235	1.38
$C_1^{(k_3)}$	-0.025	-4.5 10^{-3}	-0.021
$C_2^{(k_3)}$	-1.6 10^{-3}	1.1 10^{-3}	-0.021

in the ARIES-ST case for $-1 \leq \gamma \leq 0$ and in the ITER case for $-7 \leq \gamma \leq 0$. In the NSTX and ARIES case for values of γ smaller than the specified limit the shape of the equilibrium moves progressively away from the desired shape. The limits are not sharp transitions, but only an indicative value of the range of validity of our approximation. In the ITER case excellent approximations of the traditional plasma shape can be obtained for larger values of $-\gamma$. However, the equilibria become less realistic, since if the safety factor on axis is kept constant the plasma current decreases for increasing $-\gamma$, moving away from the target ITER values (see below). Therefore we have restricted our attention to the case $\gamma > -7$. Once again, we stress the fact that equilibria are also possible for $\gamma > 0$, but we have focused on the $\gamma < 0$ range, since it is the range more relevant to experimental tokamak equilibria.

To conclude the present discussion, we observe that a few general rules can be given for the relation between the independent parameter γ and the dependent parameters α, $\hat{k}_2$ and $\hat{k}_3$ for tokamak-like equilibria. The most important parameter is α. In general, $\alpha+\gamma \simeq 3-4$ is a good starting point for the calculation. As for the separation constants, $\hat{k}_2 \simeq 0.01 - 0.2$ and $\hat{k}_3 \simeq 1.0 - 1.4$ are fair approximations to the optimal values i.e. to the values giving the minimum distance between the equilibrium plasma shape and the input analytic shape.

Finally, we add an observation regarding the equilibria obtained with input parameters given by Eq. (25). In general, all equilibria obtained with such sets of parameters will have somewhat similar plasma characteristics, if one considers the plasma parameters I, β_t and q_*. The main variation is observed in the poloidal beta, $\beta_p = \beta_t q_*^2/\epsilon^2$. For the ITER case, which extends over the largest range of values for γ, we have calculated that for $-7 \leq \gamma \leq 0$ the plasma current varies between $6.3 \lesssim I \lesssim 10.3[MA]$, the toroidal beta between $2.0\% \lesssim \beta_t \lesssim 2.3\%$, the kink safety factor between $3.0 \lesssim q_* \lesssim 4.9$, and the poloidal beta between $1.8 \lesssim \beta_p \lesssim 5.5$. All results have been obtained by fixing the safety factor on axis, $q_{axis} = 1$. In conclusion, the equilibria obtained with the input parameters giving the optimal plasma shape mainly differ among themselves because of the value of poloidal beta.

VI Conclusions

In the present work we have presented an analytic solution to the Grad-Shafranov equation. With our solution, realistic tokamak-like equilibria can be represented by evaluating only a small number of well-known special functions. It has been shown that the method is fairly

flexible, and that equilibria with the geometry of existing and future tokamaks can be obtained. In general, once the plasma geometry (ϵ, δ, κ) has been chosen, four input parameters (γ, α, k_2, k_3) must still be assigned. Empirical relations have been presented that give $\alpha = \alpha(\gamma)$, $k_2 = k_2(\gamma)$ and $k_3 = k_3(\gamma)$ for several geometries of fusion interest.

In order to use our solution to produce an equilibrium, it is only necessary to be able to numerically evaluate Whittaker functions. In our calculations we have used the Mathematica package, in which Whittaker functions are readily available. The key step in the calculation consists of solving the system of algebraic equations (16), (17), (20) and (21), a trivial task for any numerical solver.

The analytic solution of the GS equation is useful in two respects. First, it constitutes a robust benchmark for numerical equilibrium solvers, since it can be evaluated to any desired degree of accuracy with standard numerical tools. Second, an exact equilibrium can be used as an input for the stability analysis of a tokamak. By using an exact equilibrium, no uncertainties are present in the input, and this allows for a more accurate evaluation of the error in the stability analysis, and of the convergence properties of the tools used for the stability analysis itself.

VII Acknowledgments

This research was performed under an appointment to the Fusion Energy Postdoctoral Research Program, administered by the Oak Ridge Institute for Science and Education under contract number DE-AC05-06OR23100 between the U.S. Department of Energy and Oak Ridge Associated Universities.

A Determination of the expansion coefficients

The solution is determined as follows. Assume we are given values for ϵ, κ, δ, α and γ as well as trial values for $k_{2,3}$ and correspondingly $\lambda_{2,3} = -i(\gamma - k_{2,3}^2)/(4\epsilon\sqrt{\alpha})$. Next set $k_1 = 0$ yielding $\lambda_1 = -i\gamma(/4\epsilon\sqrt{\alpha})$.

Now define $\rho_- = i\sqrt{\alpha}(1-\epsilon)^2/\epsilon$, $\rho_+ = i\sqrt{\alpha}(1+\epsilon)^2/\epsilon$, $\rho_\delta = i\sqrt{\alpha}(1-\delta\epsilon)^2/\epsilon$, and $\rho_a = i\sqrt{\alpha}(R_{axis}/R_0)^2/\epsilon$. The conditions, in the same order as they appear in the main text are given by:

$$
\begin{aligned}
&[(a_1W_1 + b_1M_1) + (a_2W_2 + b_2M_2) + (a_3W_3 + b_3M_3)]_{\rho_-} = 0 \\
&[(a_1W_1 + b_1M_1) + (a_2W_2 + b_2M_2) + (a_3W_3 + b_3M_3)]_{\rho_+} = 0 \\
&[(a_1W_1 + b_1M_1) + (a_2W_2 + b_2M_2)\cos(k_2\kappa) + (a_3W_3 + b_3M_3)\cos(k\kappa)]_{\rho_\delta} = 0 \\
&[(a_1W_1' + b_1M_1') + (a_2W_2' + b_2M_2')\cos(k_2\kappa) + (a_3W_3' + b_3M_3')\cos(k\kappa)]_{\rho_\delta} = 0 \\
&\left(\frac{1}{\rho_-}\frac{\epsilon(1-\epsilon)}{2}\right)\left[\frac{k_2^2(a_2W_2 + b_2M_2) + k_3^2(a_3W_3 + b_3M_3)}{(a_1W_1' + b_1M_1') + (a_2W_2' + b_2M_2') + (a_3W_3' + b_3M_3')}\right]_{\rho_-} \\
&\qquad = \frac{(1-\hat{\delta})^2}{\kappa^2} \\
&[(a_1W_1' + b_1M_1') + (a_2W_2' + b_2M_2') + (a_3W_3' + b_3M_3')]_{\rho_a} = 0 \\
&[(a_1W_1 + b_1M_1) + (a_2W_2 + b_2M_2) + (a_3W_3 + b_3M_3)]_{\rho_a} = 1
\end{aligned}
\tag{A.1}
$$

Here U_j denotes W_j or M_j with $U_j \equiv U_{\lambda_j,1/2}(\rho)$ and $U_j' = dU_j/d\rho$.

Note that there are seven unknowns: a_1, a_2, a_3, b_1, b_2, b_3 and ρ_a. The equations are linear in the unknowns with the exception of ρ_a. A linear solver (for the first five equations) coupled with a root finder (for the last two) makes this a trivial numerical problem for Mathematica.

References

[1] H.Grad, H. Rubin, Proc. of the 2nd United Nations Conference on the Peaceful Use of Atomic Energy, United Nations, Geneva **31**, 190 (1958)

[2] R. Lüst, A. Schlüter, Z. Naturforschung **12a**, 850 (1957)

[3] V. D. Shafranov, Reviews of Plasma Physics **2**, 103, Consultants Bureau New York-London (1966)

[4] L. S. Solov'ev, Zh. Tekh. Fiz. **53**, 626 (1967)

[5] C. V. Atanasiu, S. Günter, K. Lackner, I. G. Miron, Phys. Plasmas **11**, 3510 (2004)

[6] L. Guazzotto, R. Betti, J. Manickam and S. Kaye, Phys. Plasmas **11**, 604 (2004)

[7] M. Ono, S. M. Kaye, Y.-K. M. Peng *et al.*, Nucl. Fusion **40**, 557 (2000)

[8] M. Shimada, D. J. Campbell, V. Mukhovatov *et al.*, Nucl. Fus. **47**, S1 (2007)

[9] F. Najmabadi and the ARIES Team, Fusion Eng. Des. **65**, 143 (2003)

[10] M. Abramowitz and I. A. Stegun, *Handbook of Mathematical Functions* (Dover Publications, New York, 1964) 504-505